ORGANOMETALLICS

Article

pubs.acs.org/Organometallics

Metalated Oligosilanylstibines

Rainer Zitz,† Judith Baumgartner,*,‡ and Christoph Marschner*,†

†Institut für Anorganische Chemie, Technische Universität Graz, Stremayrgasse 9, 8010 Graz, Austria

‡Institut für Chemie, Karl Franzens Universität Graz, Stremayrgasse 9, 8010 Graz, Austria

S Supporting Information

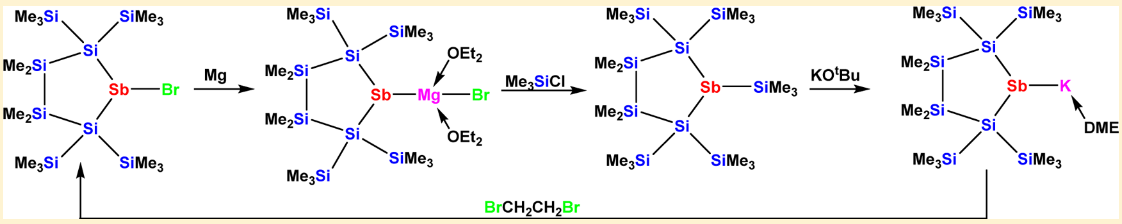

ABSTRACT: The reaction of a cyclic disilylated bromostibine with magnesium yields a rare example of a magnesium stibide that can be silylated with trimethylchlorosilane. Reaction of the thus-obtained trisilylated stibine with potassium *tert*-butoxide gives a potassium stibide in a clean reaction. Attempts to obtain an antimony-containing oligosilanide did not lead to the expected compound but to another potassium stibide, which presumably forms from the initially formed silanide by a 1,2-silyl shift. The synthetic potential of the obtained stibides to serve as building blocks could be shown by the preparation of stibylated zircono- and hafnocenes.

1. INTRODUCTION

As outlined previously,[1] silylated antimony compounds are not very abundant. If one looks for disilylated stibides, $(R_3Si)_2SbM$ (M = Li, Na, K, and Mg), it becomes obvious that the only well-known example is $(Me_3Si)_2SbLi$, prepared first by Becker et al.[2] and known as solvates with either DME or THF. Reaction of $(Me_3Si)_3Sb$ with MeLi provides convenient access to the stibide, which was shown to be extremely useful for the synthesis of a number of interesting compounds.[3−10] The analogous potassium stibide $(Me_3Si)_2SbK$ was obtained by reaction of $(Me_3Si)_3Sb$ with potassium *tert*-butoxide.[11]

Our recent study concerning oligosilanylated antimony compounds[1] presented us with the opportunity to prepare antimony-containing oligosilanides using the established protocol of removing trimethylsilyl groups by reaction with potassium *tert*-butoxide.[12−14] However, as observed previously for related phosphorus chemistry,[15] the products of such reactions are not silanides but stibides.

2. RESULTS AND DISCUSSION

Synthesis. Recently, we could show that reaction of bromostibacyclosilane **2** with potassium graphite leads to the formation of distibine **1** (Scheme 1). It is, however, not entirely clear whether this reaction involves the intermediate formation of the respective potassium stibide or is radical by nature.[16] An attempt to accomplish the same reaction with magnesium as reducing agent did not lead to the distibine but rather to respective Grignard-type magnesium stibide **3** (Scheme 1). Although magnesium stibides are a known class of compounds, the number of reported examples is still very small.[17−21] Compound **3** is not very stable, and over time in ethereal solution, it decomposes to the respective hydrostibine **4**. Freshly prepared **3**, however, is an interesting nucleophilic building block. Reaction with trimethylchlorosilane gives trisilylated stibine **5** in a clean conversion. Reaction of **5** with potassium *tert*-butoxide led to potassium stibide **6**. In an attempt to couple stibide **6** to distibine **1**, it was treated with 1,2-dibromoethane. The resulting product was, however, not distibine **1** but bromostibine **2**, which presumably was formed by metal halogen exchange. This seems to support the involvement of stibinyl radicals[16] in the formation of **1**.[1]

In an attempt to obtain a 1,2-dianionic species,[22,23] we subjected a solution of stibide **6** in benzene to the reaction with an additional equivalent of potassium *tert*-butoxide in the presence of 2 equiv of 18-crown-6. NMR spectroscopic detection of complete conversion of **6**, did, however, not indicate formation of the desired dipotassium compound. Subjecting the dark red reactive crystalline solid that could be isolated to single-crystal XRD analysis showed it to be a trimetalated Sb_7 cage coordinated by three K-18-crown-6 units. Related chemistry had been observed before by Breunig and co-workers in reactions of oligostibines with Li, Na, K, or BuLi.[24]

Reaction of distibine **1** with potassium *tert*-butoxide was carried out to ascertain whether a silanide containing a distibine might be obtained. Unfortunately, in the course of the reaction not a trimethylsilyl group was cleaved off, but the Sb−Sb bond was split (Scheme 2).

Tris(trimethylsilyl)silylated stibine **7**, which can also be obtained from **2**,[1] was treated with potassium *tert*-butoxide in order to obtain an antimony containing silanide. It was expected that a trimethylsilyl group would be abstracted either

Received: December 18, 2014
Published: April 10, 2015

Scheme 1. Formation of Stibides 3 and 6 from Bromostibine 2

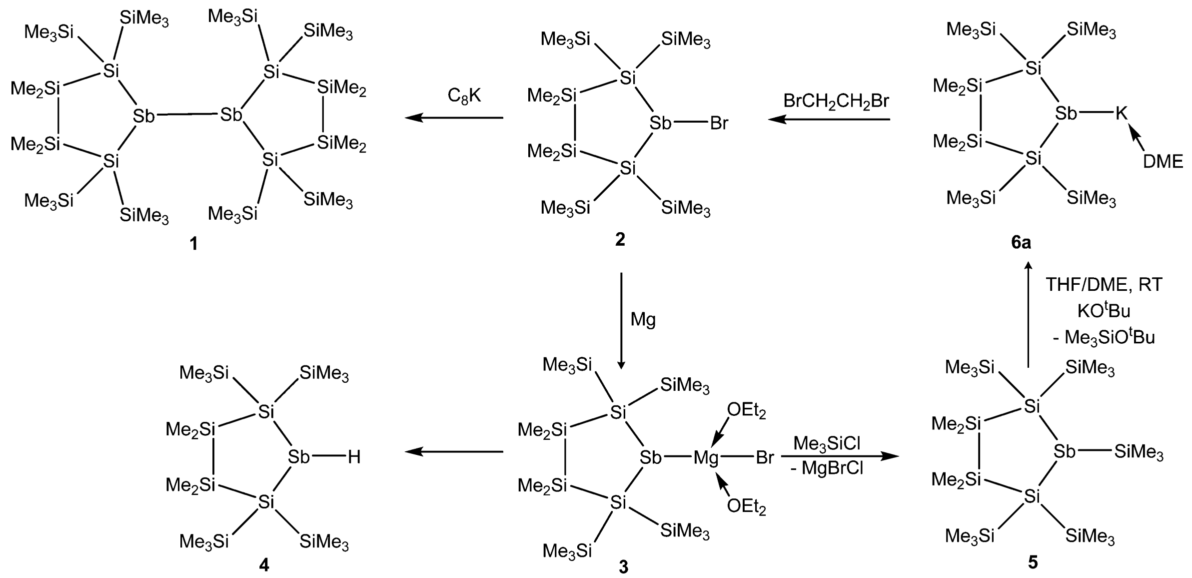

Scheme 2. Stibide Formation by Sb–Sb Bond Cleavage of 1 with Potassium *tert*-Butoxide

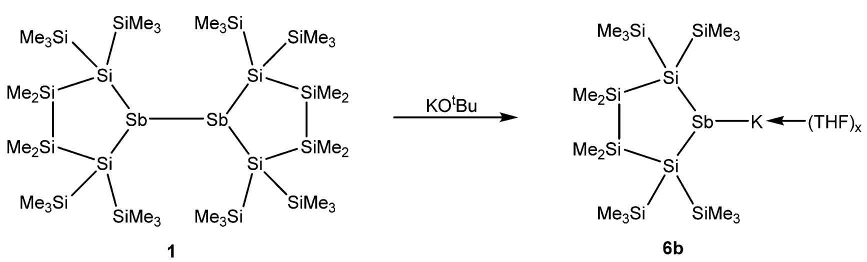

Scheme 3. Formation of Potassium Stibide 8 via a Transient Silanide

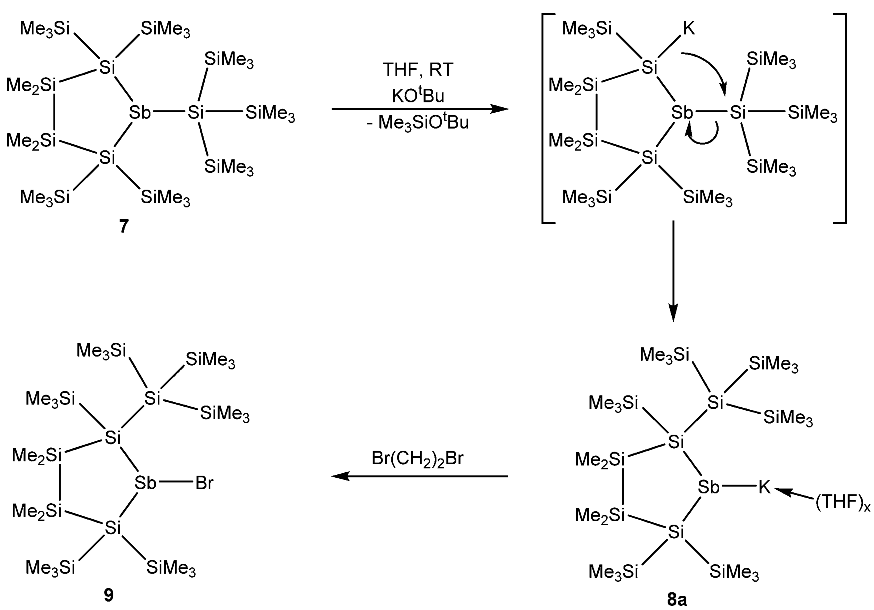

from the cyclic part or the tris(trimethylsilyl)silyl group attached to antimony. The ^{29}Si NMR spectrum of obtained compound **8** showed eight different silicon resonances, indicating attack of the alkoxide onto a trimethylsilyl group attached to the cyclosilane unit. However, none of the resonances displayed the typical upfield shift characteristic for anionic silicon atoms. It was therefore concluded that the tris(trimethylsilyl)silyl group underwent a subsequent 1,2 shift to give stibide **8** (Scheme 3). An attempt to silylate **8** with tris(trimethylsilyl)silyl chloride was not successful. Reaction of **8** with 1,2-dibromoethane gave bromostibine **9** (Scheme 3) in the same way as **2** was obtained from **6**.

The number of known stibylated group 4 metallocenes is quite small.[25−31] The few known titanocenes were obtained by

DOI: 10.1021/om501297h
Organometallics 2015, 34, 1431−1439

Scheme 4. Formation of Stibylated Group 4 Metallocenes

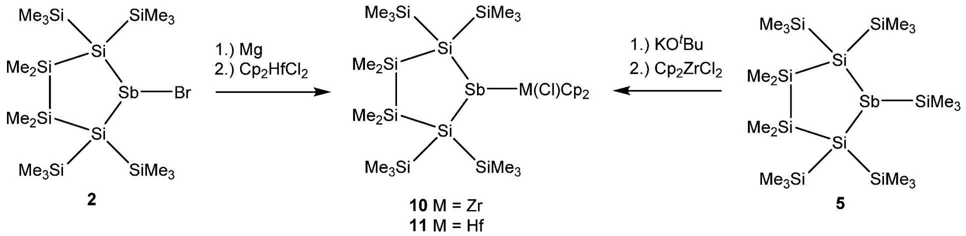

Table 1. NMR Spectroscopic Data of Oligosilanylstibyl Compounds[a]

compound	^{1}H ($SiMe_3$)	^{1}H ($SiMe_2$)	^{13}C ($SiMe_3$)	^{13}C ($SiMe_2$)	^{29}Si ($SiMe_3$)	^{29}Si ($SiMe_2$)	^{29}Si (Si_q)
3	0.34	0.37	2.8	−1.7	−10.8	−20.3	−125.9
4	0.31/0.30	0.34	2.4/2.0	−1.3/−2.1	−6.2/−9.0	−14.8	−119.2
5	0.39/0.59(Sb−SiMe$_3$)	0.40	3.0/6.4 (Sb−SiMe$_3$)	−1.6	−8.7/−9.4(Sb−SiMe$_3$)	−20.4	−124.0
6	0.43	0.53	2.7	−1.5	−14.2	−19.0	−125.2
8	0.49 (36H) /0.44/0.40	0.61/0.58/ 0.57/0.54	4.9 (3× SiMe$_3$) /3.6/3.3/3.0	0.5/0.3/ 0.2/0.1	−9.3 (3× SiMe$_3$)/−14.0/−14.7/−16.2	−18.8/−19.2	−122.4/−124.4/−126.4
9	0.52/0.47/ 0.39 (27H) /0.33	0.52/0.47/ 0.32/0.30	5.5/4.5/3.4	1.1/0.9/ 0.4/0.1	0.7/−0.2/−8.2/−9.3	−11.5/−14.8	−93.9/−100.6/−121.7
10	0.50	0.44	3.5	−1.1	−8.1	−20.4	−103.7
11	0.51	0.46	3.6	−1.0	−8.1	−19.9	−109.7

[a]Chemical shifts in ppm in reference to TMS.

employing Cp_2Ti(btmsa) in reactions with distibines[25,26] or dihydrostibines.[27] Tilley and Waterman studied stibylated CpCp*Hf compounds. Reaction of CpCp*$HfCl_2$ with $LiSbMes_2$ was found to give a distibylated complex,[28] whereas a stibylidene complex was obtained from the reaction of CpCp*Hf(Me)OTf with LiSb(H)Mes.[29] That a Hf−Sb bond can even be formed in a σ-bond metathesis reaction was shown for the conversion of CpCp*Hf(Cl)H with $MesSbH_2$.[30] The only known stibyl zirconocene was prepared by reaction of Ph_2SbLi with Cp_2ZrCl_2.[31] The utility of stibides **3** and **6** for the synthesis of group 4 stibyl compounds was also investigated. Reaction of **5** with KO*t*-Bu, and further on with zirconocene dichloride, led to stibyl zirconocene compound **10** (Scheme 4). However, under the same conditions, reaction with hafnocene dichloride resulted in a complex inseparable mixture of products. Switching to magnesium stibide **3**, generated in situ from bromostibacyclosilane **2** with magnesium, reaction with hafnocene dichloride gave stibylhafnocene chloride **11** in a clean reaction (Scheme 4).

Attempts to obtain distibylated titanocenes by reaction of Cp_2Ti(btmsa) with **1** or related distibines[1] were not successful. Also, the addition of an additional equivalent of **6** to **10** or **11** did not lead to distibylated metallocenes. The reason for these failures is likely the steric bulk of the oligosilanylated stibyl units.

NMR Spectroscopy. ^{1}H and ^{13}C NMR spectroscopic characterization of the stibasilanes is particularly useful with respect to molecular symmetry and purity (Table 1). As the spectral windows of chemical shifts of silylated methyl groups are very small for ^{1}H and ^{13}C NMR, the observed values are not particularly meaningful, and information concerning the molecular structure can mainly be derived from ^{29}Si NMR spectra. Chemical shifts of the ^{29}Si resonances can usually rather easily be assigned to a particular substitution pattern (Table 1).[32] The compounds described in this study all share the structural unit of a stibacyclopentasilane. The comparison of the spectroscopic properties of these and related compounds[1] reveals two different groups of compounds. The first group, featuring more electronegative exocyclic substituents at the antimony atom, exhibits configurational stability of the antimony atom. This group includes bromostibines **2** and **9**, hydrostibine **4**, and a related *tert*-butoxystibine.[1] The configurational stability of the antimony atom allocates the exocyclic substituent on one side of the cyclosilane ring and thus diminishes the symmetry of the molecule. Two different resonances for trimethylsilyl groups (being either on the same side of the exocyclic substituent or on the other one) are found for these molecules. A more unexpected observation was that the compounds with electronegative substituents also share a downfield shift of the ^{29}Si NMR resonances of the $SiMe_2$ groups to values between −11.5 and −17.8 ppm. The second group of compounds, with more electropositive substituents (silyl groups and metals), lacks configurational stability of the antimony atom and includes stibides **3**, **6**, and **8**, stibylated metallocenes **10** and **11**, trisilylated stibines **5** and **7**, and distibine **1**. For these compounds, a fast pyramidal inversion at the Sb atom renders the trimethylsilyl groups magnetically equivalent on the NMR time scale. This behavior is consistent with a recent computational study that showed pyramidal inversion to be strongly dependent on substituent electronegativity and sterics. It was shown that SbH_3 (E^{inv} = 182 kJ mol^{-1}) and $SbMe_3$ (E^{inv} = 228 kJ mol^{-1}) are clearly configurationally stable, whereas the calculated inversion barrier for $Sb(SiH_3)_3$ is comparably low (E^{inv} = 92 kJ mol^{-1}) because of stabilization of the planar transition state by electrostatic and hyperconjugational effects.[1] Studying the pyramidal inversion processes of antimony atoms incorporated into the stibacyclopentasilane unit showed that the barrier for compound **5** is as low as 47 kJ mol^{-1}. For such a small barrier, the inversion process is certainly expected to be fast at ambient temperature.[1]

The trimethylsilyl resonances for the metalated stibides are markedly shifted to high field, dependent on the electropositive character of the metal. Shifts around −14 ppm were observed for potassium stibides **6** and **8**, whereas for magnesium stibide

DOI: 10.1021/om501297h
Organometallics 2015, 34, 1431−1439

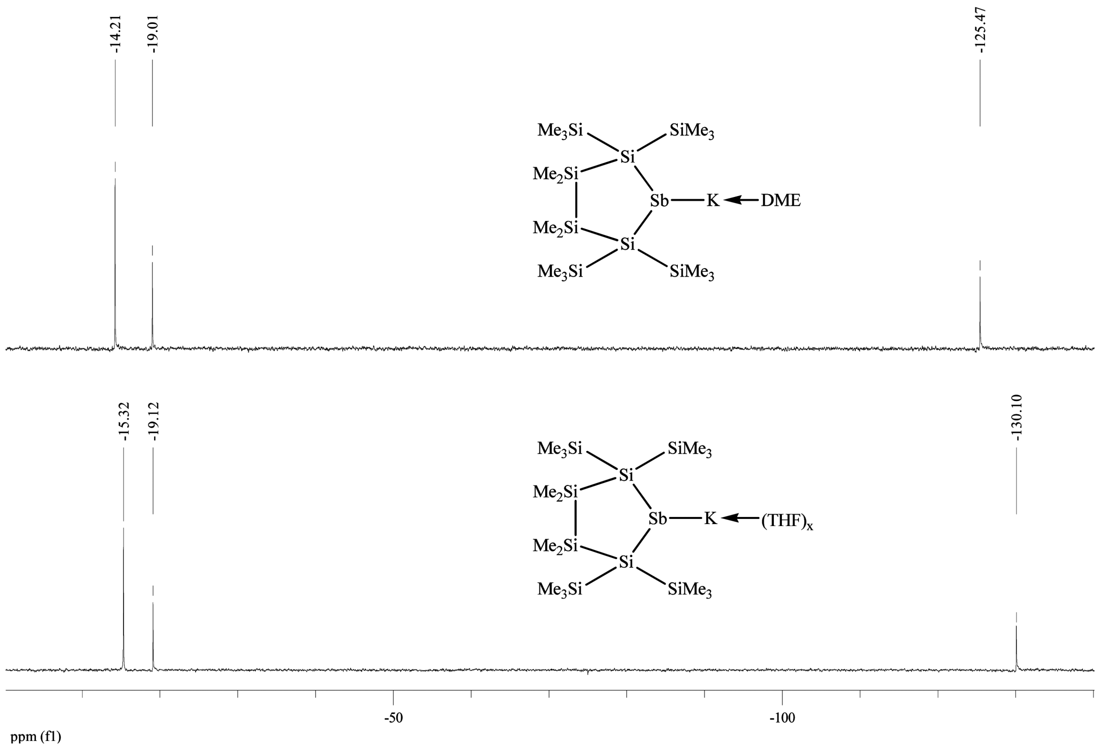

Figure 1. ^{29}Si NMR spectra of potassium stibide **6a,b** in DME or THF.

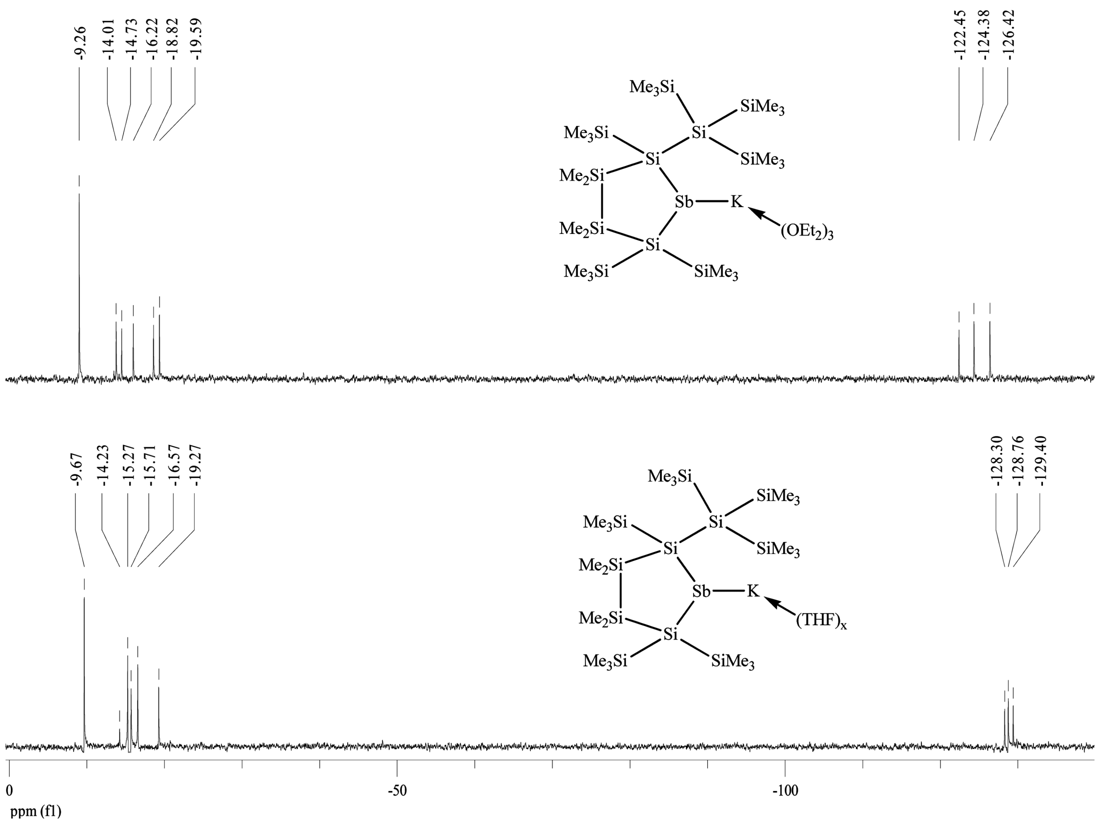

Figure 2. ^{29}Si NMR spectra of asymmetric potassium stibide **8** in Et_2O or THF.

3, the respective resonance can be found at −10.8 ppm. For metallocenes **10** and **11**, the trimethylsilyl resonances at −8.1 ppm are in the same range as those found for silylated compounds **5** and **7**. The $SiMe_2$ resonances of the second group are all located between −19.0 and −23.3 ppm.

The strongly asymmetric structure of compounds like bromostibine **9** causes a large number of ^{29}Si NMR resonances. Straightforward assignment of the ^{29}Si NMR spectrum for such compounds was not possible; therefore, the use of 2D spectroscopic methods proved useful, in particular hetero-

DOI: 10.1021/om501297h
Organometallics 2015, 34, 1431−1439

nuclear correlation spectroscopy. Figures S1 and S2 show typical $^{1}H-^{29}Si$ and $^{1}H-^{13}C$ correlation spectra. The respective signal assignments are given in Table S3. The 2D experiments of **9** also show overlapping of two signals of trimethylsilyl groups (signals 1 and 4) in the ^{13}C NMR spectrum and of the signals of a dimethylsilyl and a trimethylsilyl group (signals 2 and 6) in the ^{1}H NMR spectrum. For complete signal assignment, additional 1D-NOESY experiments were carried out. Figure S3 shows the structure of **9** with the signal assignment and the NOESY results.

For stibides **6** and **8**, the ^{29}Si NMR spectra in ethereal solvents are different. In particular, the signals corresponding to the quaternary silicon atoms respond strongly to different coordinating solvents (Figures 1 and 2). For **8** in Et_2O, the signals are in a range of $\delta = -122$ to -126 ppm, whereas in the THF solution, the signals are clustered in the range of $\delta \approx -128$ to -129 ppm. Thus, a surprising $\Delta\delta$ of some 6.0 ppm was observed for different ethereal solvents. A comparison of solutions of **6** in THF and DME reveals a quite similar result. The signals for the quaternary silicon atoms show a difference of $\Delta\delta = 4.6$ ppm.

Crystal Structure Analysis. Molecular structures of antimony compounds **3** (Figure 3), **4** (Figure 4), **5** (Figure 5), **6** (Figure 6), **10** (Figure 7), and **11** (Figure 8) in the solid state could be determined by means of single-crystal XRD (Tables S1 and S2). A compilation of the obtained data is given in Table 2.

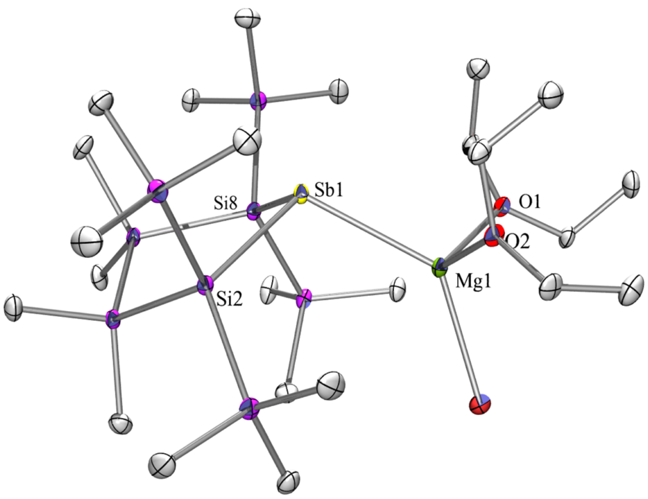

Figure 3. Molecular structure of **3** (thermal ellipsoid plot drawn at the 30% probability level). All hydrogen atoms are omitted for clarity (bond lengths in angstroms, angles in degrees). Sb(1)−Si(8) 2.5739(11), Sb(1)−Si(2) 2.5883(12), Sb(1)−Mg(1) 2.7806(13), Si(1)−Si(2) 2.3495(14), Si(3)−C(3) 1.874(4), Br(1)−Mg(1) 2.4418(13), Mg(1)−O(1) 2.038(3), Mg(1)−O(2) 2.049(3), O(1)−C(1) 1.452(4), Si(8)−Sb(1)−Si(2) 99.82(3), Si(8)−Sb(1)−Mg(1) 109.08(4), Si(2)−Sb(1)−Mg(1) 106.38(3), Br(1)−Mg(1)−Sb(1) 133.62(5).

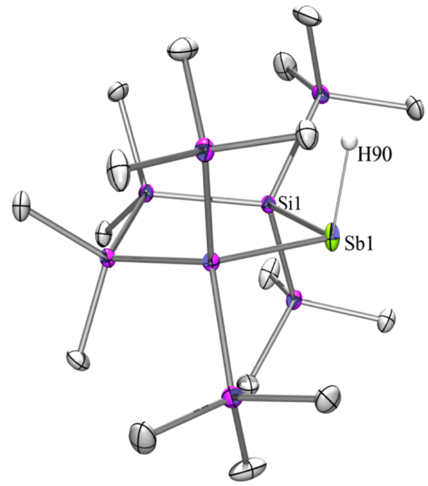

Figure 4. Molecular structure of **4** (thermal ellipsoid plot drawn at the 30% probability level). All calculated hydrogen atoms are omitted for clarity (bond lengths in angstroms, angles in degrees). Sb(1)−Si(1) 2.5919(5), Si(1)−Si(4) 2.3442(8), Si(1)−Si(2) 2.3538(7), Si(2)−C(1) 1.8861(16), Si(1)−Sb(1)−Si(1A) 98.59(2), Si(4)−Si(1)−Sb(1) 106.01(2), Si(3)−Si(1)−Sb(1) 103.43(2), Si(2)−Si(1)−Sb(1) 109.87(2).

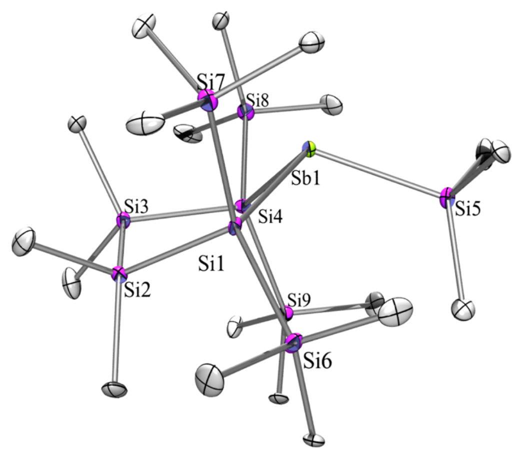

Figure 5. Molecular structure of **5** (thermal ellipsoid plot drawn at the 30% probability level). All hydrogen atoms are omitted for clarity (bond lengths in angstroms, angles in degrees). Sb(1)−Si(5) 2.570(2), Sb(1)−Si(4) 2.582(3), Sb(1)−Si(1) 2.601(3), Si(1)−Si(7) 2.345(4), Si(1)−Si(6) 2.357(4), Si(2)−C(1) 1.872(10), Si(5)−Sb(1)−Si(4) 110.80(9), Si(5)−Sb(1)−Si(1) 106.31(8), Si(4)−Sb(1)−Si(1) 100.26(8), Si(7)−Si(1)−Sb(1) 96.02(11), Si(6)−Si(1)−Sb(1) 123.79(12), Si(2)−Si(1)−Sb(1) 106.61(11).

Magnesium compound **3** (Figure 3) crystallized in the monoclinic space group $P2(1)/c$ with two molecules in the asymmetric unit. It constitutes the first solved structure with a Sb−Mg bond, and the distance of 2.7806(13) Å between the two atoms is reasonable. Potassium compound **6** (Figure 6) crystallized in the triclinic space group $P\bar{1}$ with two half molecules in the asymmetric unit. Each molecule consists of two stibacyclopentasilane rings and two potassium atoms bridging the antimony atoms. One DME molecule is coordinating to each potassium atom, and for one of the two molecules, the DME is disordered in the ethylene bridge. The potassium−antimony distance is 3.5320(9) Å, in good accordance to the few comparable structures known in the literature (3.566,[33] 3.686,[24] and 3.618[34] Å), although none of these displays the structural element of a four-membered ring. This Sb−K−Sb−K ring is planar, whereas the stibacyclopentasilane rings both engage in envelope conformations with one of the $SiMe_2$ groups on the flap. The same conformational preference was also found for the stibacyclopentasilane units of **3**−**5**. For **4** (Figure 4), which crystallizes in the monoclinic space group $P2/n$, the hydrogen on the antimony was located and found to be split over two positions. The Sb−H distance is with 1.71 Å, in good agreement to comparable published

DOI: 10.1021/om501297h
Organometallics 2015, 34, 1431−1439

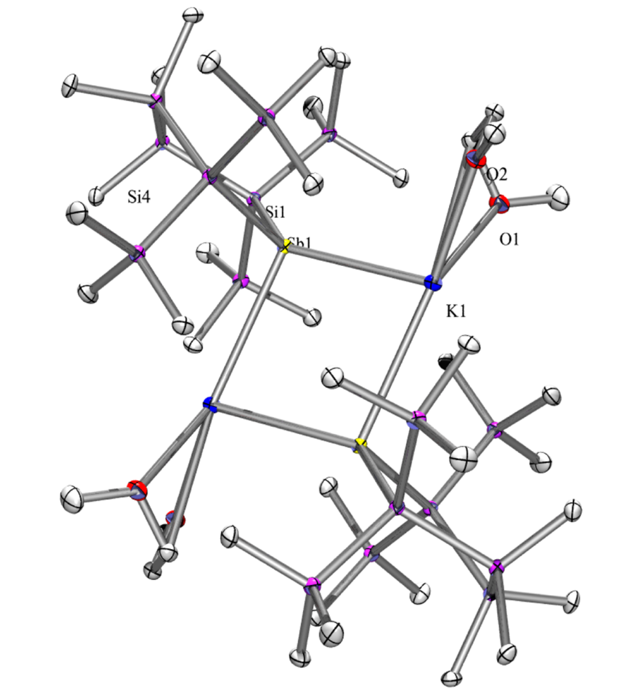

Figure 6. Molecular structure of **6** (thermal ellipsoid plot drawn at the 30% probability level). All hydrogen atoms are omitted for clarity (bond lengths in angstroms, angles in degrees). Sb(1)−Si(1) 2.5576(10), Sb(1)−Si(4) 2.5657(10), Sb(1)−K(1) 3.5320(9), Si(1)−Si(2) 2.3495(11), Si(2)−C(1) 1.891(2), K(1)−O(1) 2.6948(18), Si(1)−Sb(1)−Si(4) 97.78(3), Si(1)−Sb(1)−K(1) 134.08(2), Si(4)−Sb(1)−K(1) 113.24(3), Sb(1)−K(1)−Sb(1A) 81.09(3).

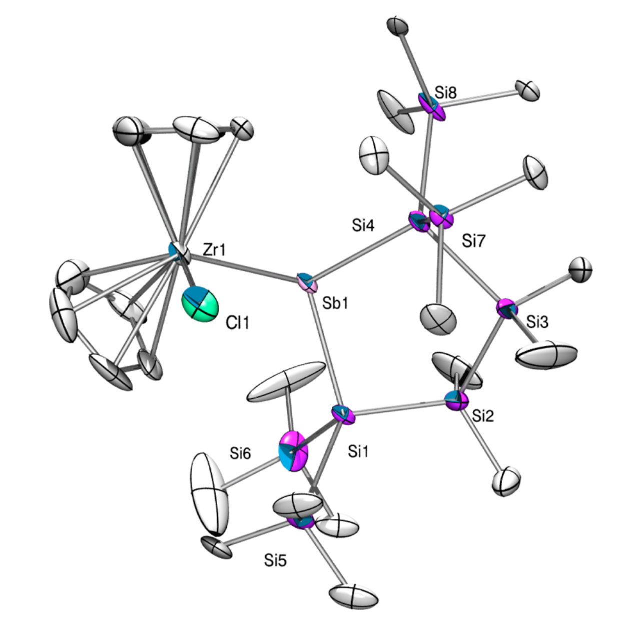

Figure 7. Molecular structure of **10** (thermal ellipsoid plot drawn at the 30% probability level). All hydrogen atoms are omitted for clarity (bond lengths in angstroms, angles in degrees). Si(2)−C(12) 1.83(3), Si(2)−C(11) 1.906(17), Si(2)−Si(1) 2.324(6), Zr(1)−Cl(1) 2.435(2), Zr(1)−Sb(1) 2.9105(10), Sb(1)−Si(4) 2.5790(18), Sb(1)−Si(1) 2.582(2), Si(3)−Si(2)−Si(1) 112.5(4), Cl(1)−Zr(1)−Sb(1) 104.46(7), Si(4)−Sb(1)−Si(1) 102.44(6), Si(4)−Sb(1)−Zr(1) 116.30(5), Si(1)−Sb(1)−Zr(1) 117.73(5).

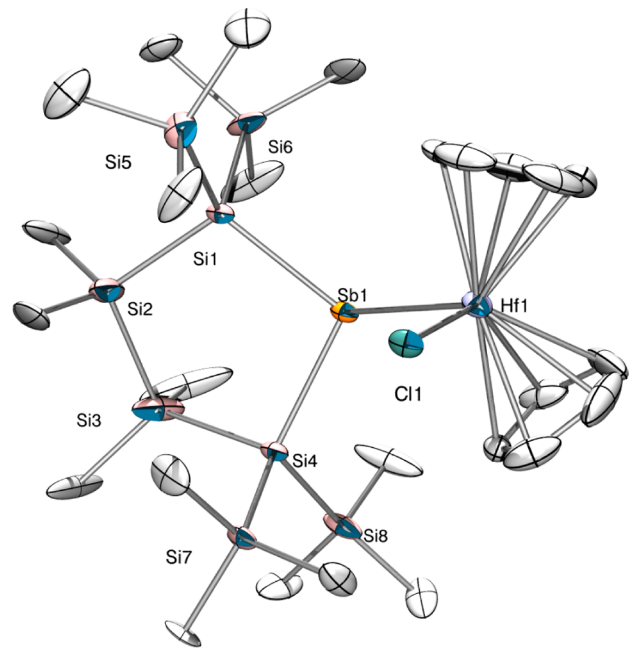

Figure 8. Molecular structure of **11** (thermal ellipsoid plot drawn at the 30% probability level). All hydrogen atoms are omitted for clarity (bond lengths in angstroms, angles in degrees). Hf(1)−Cl(1) 2.470(2), Hf(1)−Sb(1) 2.8871(9), Sb(1)−Si(4) 2.576(2), Sb(1)−Si(1) 2.577(3), Si(2)−Si(1) 2.345(8), Si(2)−C(12) 1.88(3), Si(3)−Si(2)−Si(1) 106.5(5), Cl(1)−Hf(1)−Sb(1) 104.75(6), Si(4)−Sb(1)−Si(1) 102.41(8), Si(4)−Sb(1)−Hf(1) 116.19(6), Si(1)−Sb(1)−Hf(1) 117.78(6), Si(8)−C(24)−Si(88) 27.8(3).

structures.[35,36] The Si−Sb distances in all compounds range from 2.56 to 2.60 Å and are slightly longer than the mean range of 2.56 Å obtained from a search in the Cambridge Crystallographic Database.[37] In trimethylsilylated compound **5** (Figure 5), which crystallized in the monoclinic space group *P*2(1) with two molecules in the asymmetric unit, no differences between exo- and endocyclic Sb−Si distances could be observed.

Antimony group 4 compounds **10** (Figure 7) and **11** (Figure 8) both crystallize in the orthorhombic space group *Pbca*. **10** represents the first example of a solid-state structure with a Zr−Sb bond; although three comparable examples of Hf−Sb compounds are already known,[28−30] none of them contains a Hf−Sb−Si unit. The bond length of 2.8871(9) Å for Sb−Hf is comparable to the two reported ones.[28,29]

NMR spectroscopic indication of compounds with or without configurational stability can be well-correlated with the pyramidality of the antimony atom, which can be expressed in terms of the sum of angles around antimony. Compounds with configurational stability such as **2**, **4**, and the related *tert*-butoxystibine[1] feature more pyramidalized stibines with values between 293 and 298°. The respective compounds with more electropositive substituents show more flattened antimony atoms. The sum of angles around antimony ranges from 317° for a trimethylsilyl substituent (**5**) to values around 336.4° for stibylated metallocenes **10** and **11** (Table 2).

3. CONCLUSIONS

The current account is an extension of our recent study concerning oligosilanylated antimony compounds.[1] It deals mainly with metalated examples of a 2,2,5,5-tetrakis-(trimethylsilyl)-3,3,4,4-tetramethylstibacyclopentasilane. The

DOI: 10.1021/om501297h
Organometallics 2015, 34, 1431−1439

Table 2. Compilation of Structural Data Derived by Single-Crystal XRD Analysis

compound	d_{Sb-X} (Å)	d_{Si-Sb} (Å)	$d_{Si-SiMe_3}$ (Å)	$d_{Si-SiMe_2}$ (Å)	$\Sigma\angle_{Sb}$ (deg)	$\angle_{SiSbSi}$ (deg)	$\angle_{SiSbX}$ (deg)
3 (X = Mg)	2.7806(13)	2.5883(12), 2.5739(11)	2.332(2)–2.357(2)	2.3495(14), 2.3467(14)	315.28(3), 318.07(4)	99.82(3)	109.08(4), 106.38(3)
4 (X = H)	1.71(4)	2.5919(6), 2.5919(5)	2.3442(8), 2.3458(8)	2.3538(7)	293	98.59(2)	98.3(5), 96.5(5)
5 (X = Si)	2.570(2)	2.582(3), 2.601(3)	2.345(4)–2.361(4)	2.356(4), 2.360(3)	317.36(9), 317.26(9)	100.26(8)	110.80(9), 106.31(8)
6 (X = K)	3.5320(9), 3.5624(11)	2.5549(9)–2.5653(11)	2.3383(11)–2.3464(10)	2.3495(11), 2.3519(11)	n.a.	97.78(3), 97.68(3)	134.08(2), 113.24(3), 109.65(3), 98.14(2)
10 (X = Zr)	2.9105(10)	2.582(2), 2.5790(18)	2.308(4)–2.428(4)	2.324(6), 2.411(8)	336.47(6)	102.44(6)	116.30(5), 117.73(5)
11 (X = Hf)	2.8871(9)	2.576(2), 2.577(3)	2.330(5)–2.425(5)	2.345(8), 2.302(11)	336.38(8)	102.41(8)	116.19(6), 117.78(6)

reaction of respective bromostibine **2** with magnesium occurs in a Grignard-type reaction, leading in a clean reaction to a stibyl magnesium bromide (**3**). The compound was isolated as etherate and can be used as nucleophilic building block that is easily silylated with trimethylchlorosilane. The obtained trimethylsilylated stibine **5** reacts with potassium *tert*-butoxide to yield cleanly a potassium stibide (**6**). Another potassium stibide (**8**) was formed in the reaction of the tris(trimethylsilyl)silylated derivative of the stibacyclopentasilane with potassium *tert*-butoxide. We assume that the initial attack of the alkoxide occurs on one of the trimethylsilyl groups of the ring. In a 1,2-silyl shift, the tris(trimethylsilyl)silyl group migrates to the anionic silicon atom, leading to the formation of a stibide. Similar reactivity is already known for oligosilanylated phosphines[15,38] and likely reflects the increased ability to stabilize a negative charge of antimony compared to silicon.

The potential of the obtained stibides to serve as building blocks for stibylated early transition metal compounds could be demonstrated by the synthesis of stibylated zircono- and hafnocenes (**10**, **11**).

4. EXPERIMENTAL SECTION

General Remarks. All reactions involving air-sensitive compounds were carried out under an atmosphere of dry nitrogen or argon using either Schlenk techniques or a glovebox. All solvents were dried using a column-based solvent purification system.[39] Compounds **1**, **2**, and **7** were prepared according to previously published procedures.[1] All other chemicals were obtained from different suppliers and used without further purification.

^{1}H (300 MHz), ^{13}C (75.4 MHz), and ^{29}Si (59.3 MHz) NMR spectra were recorded on a Varian INOVA 300 spectrometer. If not noted otherwise, for all samples benzene-d_6 was used or, in the case of reaction samples, they were measured with a water-d_2 capillary in order to provide an external lock frequency signal. To compensate for the low isotopic abundance of ^{29}Si, the INEPT pulse sequence was used for the amplification of the signal.[40,41] Elemental analysis was carried out using a Heraeus VARIO ELEMENTAR instrument.

X-ray Structure Determination. For XRD analyses, the crystals were mounted onto the tip of glass fibers, and data collection was performed with a BRUKER-AXS SMART APEX CCD diffractometer using graphite-monochromated Mo Kα radiation (0.71073 Å). The data were reduced to F^2_o and corrected for absorption effects with SAINT[42] and SADABS,[43] respectively. The structures were solved by direct methods and refined by full-matrix least-squares method (SHELXL97).[44] If not noted otherwise, all non-hydrogen atoms were refined with anisotropic displacement parameters. All hydrogen atoms were located in calculated positions to correspond to standard bond lengths and angles. Crystallographic data (excluding structure factors) for the structures of compounds **3**–**6**, **10**, and **11** reported in this paper have been deposited with the Cambridge Crystallographic Data Center as CCDC-1027151 (**3**), -1027152 (**4**), -1008599 (**5**), -1027153 (**6**), -1027155 (**10**), and -1027154 (**11**) and can be obtained free of charge at http://www.ccdc.cam.ac.uk/products/csd/request/.

*2,2,5,5-Tetrakis(trimethylsilyl)-1-stibatetramethylcyclopentasilanyl magnesium bromide·(OEt$_2$)$_2$ (**3**).* To a solution of **2** (70 mg, 0.105 mmol) in Et_2O (3 mL) was added magnesium turnings (40 mg, 0.158 mmol), followed by stirring at room temperature for 2 h. After a few minutes, a color change from light red to deep red was observed. To remove excess Mg, the solution was filtered over Celite, and the insoluble residue was washed with Et_2O. Slow evaporation of the solvent at room temperature provided **3** (65 mg, 93%) as brownish plates. ^{1}H NMR (δ ppm): 3.23 (q, $^{3}J_{H-H}$ = 7.0 Hz, Et_2O), 1.04 (t, $^{3}J_{H-H}$ = 7.0 Hz, Et_2O), 0.37 (s, 12H, $SiMe_2$), 0.34 (s, 36H, $SiMe_3$). ^{13}C NMR (δ ppm): 65.91 [$(CH_3CH_2)_2O$], 15.48 [$(CH_3CH_2)_2O$], 2.84 ($SiMe_3$), −1.71 ($SiMe_2$). ^{29}Si NMR (δ ppm): −10.8 ($SiMe_3$), −20.3 ($SiMe_2$), −125.9 (Si_q).

*1-Hydro-2,2,5,5-tetrakis(trimethylsilyl)-1-stibatetrametylcyclopentasilane (**4**).* Over a duration of 14 days, a solution of **3** (65 mg, 0.077 mmol) in Et_2O (2 mL) decomposed quantitatively to hydrostibine **4**. After removal of the solvent under vacuum, the residue was dissolved in pentane and filtered over Celite. **4** (28 mg, 62%) was isolated as colorless crystals obtained from pentane at −37 °C. Mp: 126–128 °C. ^{1}H NMR (δ ppm): 0.34 (s, 12H, $SiMe_2$), 0.31 (s, 18H, $SiMe_3$), 0.30 (s, 18H, $SiMe_3$). ^{13}C NMR (δ ppm): 2.35 ($SiMe_3$), 2.02 ($SiMe_3$), −1.32 ($SiMe_2$), −2.10 ($SiMe_2$). ^{29}Si NMR (δ ppm): −6.2 ($SiMe_3$), −9.0 ($SiMe_3$), −14.8 ($SiMe_2$), −119.2 (Si_q). Anal. Calcd for $C_{16}H_{49}SbSi_8$ 588.00: C 32.68, H 8.40. Found: C 31.54, H 7.96.

*1,2,2,5,5-Pentakis(trimethylsilyl)-1-stibatetramethylcyclopentasilane (**5**).* To a solution of **2** (78 mg, 0.117 mmol) in Et_2O (2 mL) magnesium turnings (4 mg, 0.176 mmol) were added and stirred for 2 h. The solution was filtered to remove excess magnesium, and trimethylchlorosilane (13 mg, 0.117 mmol) was added. After 12 h, the reaction was complete (detected by NMR spectroscopy), and the solvent was removed. The residue was treated with pentane three times and filtered over Celite. Orange-brown crystalline **5** (55 mg, 71%) was obtained by crystallization from pentane at −37 °C after 48 h. Mp: 182–184 °C. ^{1}H NMR (δ ppm): 0.59 (s, 9H,

DOI: 10.1021/om501297h
Organometallics 2015, 34, 1431–1439

$SbSiMe_3$), 0.40 (s, 12H, $SiMe_2$), 0.39 (s, 36H, $SiMe_3$). ^{13}C NMR (δ ppm): 6.39 (Me_3Si-Sb), 2.99 (Me_3Si-Si_q), −1.56 (Me_2Si). ^{29}Si NMR (δ ppm): −8.7 (Me_3Si-Si_q), −9.4 (Me_3Si-Sb), −20.4 (Me_2Si), −124.0 (Si_q). Anal. Calcd for $C_{19}H_{57}SbSi_9$ 660.19: C: 34.57, H: 8.70. Found: C: 34.63, H: 8.33. UV: λ_1 = 275 nm, $\varepsilon_1 = 2.4 \times 10^4$ l $mol^{-1}cm^{-1}$.

*2,2,5,5-Tetrakis(trimethylsilyl)-1-stibatetramethylcyclopentasilan-1-yl potassium·DME (**6**).* **5** (60 mg, 0.091 mmol) and KO*t*-Bu (11 mg, 0.095 mmol) were dissolved in THF (3 mL) and stirred for 12 h (reaction control by NMR). The solvent was removed under vacuum, and the precipitate was treated with Et_2O/DME 5:1. Slow evaporation afforded orange-red crystalline **6** (61 mg, 94%). ^1H NMR (δ ppm): 3.05 (s, 6H, DME), 3.00 (s, 4H, DME), 0.53 (s, 12H, $SiMe_2$), 0.43 (s, 36H, $SiMe_3$). ^{13}C NMR (δ ppm): 71.23 (DME), 58.88 (DME), 2.73 (Me_3Si), −1.51 (Me_2Si). ^{29}Si NMR (δ ppm): −14.2 (Me_3Si), −19.0 (Me_2Si), −125.2 (Si_q).

*2,5,5-Tris(trimethylsilyl)-2-[tris(trimethylsilyl)silyl]-1-stibatetramethylcyclopentasilan-1-yl-potassium·$(Et_2O)_3$ (**8**).* KO*t*-Bu (7 mg, 0.006 mmol) and **7** (50 mg, 0.006 mmol) were dissolved in THF (2 mL) and stirred at room temperature for 3 h (reaction control by NMR). The solvent was removed, and the residue was dissolved in pentane (2 mL) with a few drops of Et_2O. After 48 h at −37 °C, red crystalline **8** (46 mg, 91%) was obtained. ^1H NMR (δ ppm): 3.20 (q, $^3J_{H-H}$ = 7.0 Hz, Et_2O), 1.05 (t, $^3J_{H-H}$ = 7.0 Hz, Et_2O), 0.61 (s, 3H, $SiMe_2$), 0.58 (s, 3H, $SiMe_2$), 0.57 (s, 3H, $SiMe_2$), 0.54 (s, 3H, $SiMe_2$), 0.49 (s, 36H, $SiMe_3$), 0.44 (s, 9H, $SiMe_3$), 0.40 (s, 9H, $SiMe_3$). ^{13}C NMR (δ ppm): 4.94 ($Si(SiMe_3)_3$), 3.61 ($SiMe_3$), 3.33 ($SiMe_3$), 3.03 ($SiMe_3$), 0.47 ($SiMe_2$), 0.30 ($SiMe_2$), 0.16 ($SiMe_2$), 0.12 ($SiMe_2$). ^{29}Si NMR (δ ppm): −9.3 ($SiMe_3$), −14.0 ($SiMe_3$), −14.7 ($SiMe_3$), −16.2 ($SiMe_3$), −18.8 ($SiMe_2$), −19.6 ($SiMe_2$), −122.4 (Si_q), −124.4 (Si_q), −126.4 (Si_q).

*1-Bromo-2,5,5-tris(trimethylsilyl)-2-[tris(trimethylsilyl)silyl]-1-stibatetramethylcyclopentasilane (**9**).* KO*t*-Bu (26 mg, 0.220 mmol) and **7** (185 mg, 0.231 mmol) were dissolved in THF (4 mL) and stirred for 12 h (reaction control by NMR). The reaction mixture was added dropwise to a solution of 1,2-dibromoethane (50 mg, 0.265 mmol) in THF (3 mL). Reaction control after 5 h of stirring showed complete conversion to **9**. The solvent was removed and the remaining solid extracted three times with pentane (5 mL each). The solution was concentrated to 2 mL and stored for 15 h at −37 °C, affording red crystalline **9** (149 mg, 81%). Mp: 140−142 °C. ^1H NMR (δ ppm): 0.52 (s, 12H, $SiMe_3$, $SiMe_2$), 0.49 (s, 3H, $SiMe_2$), 0.47 (s, 9H, $SiMe_3$), 0.39 (s, 27H, $SiMe_3$), 0.33 (s, 9H, $SiMe_3$), 0.32 (s, 3H, $SiMe_2$), 0.30 (s, 3H, $SiMe_2$). ^{13}C NMR (δ ppm): 5.49 ($SiMe_3$), 4.47 ($Si(SiMe_3)_3$), 3.35 ($SiMe_3$), 1.07 ($SiMe_2$), 0.94 ($SiMe_2$), 0.39 ($SiMe_2$), 0.13 ($SiMe_2$). ^{29}Si NMR (δ ppm): 0.7 ($SiMe_3$), −0.2 ($SiMe_3$), −8.2 ($SiMe_3$), −9.3 ($SiMe_3$), −11.5 ($SiMe_2$), −14.8 ($SiMe_2$), −93.9 (Si_q), −100.6 (Si_q), −121.7 (Si_q). Anal. Calcd for $C_{22}H_{66}BrSbSi_{11}$ 841.36: C: 31.41, H: 7.91. Found: C: 31.66, H 8.02.

*Bis(cyclopentadienyl)(2,2,4,4-tetrakis(trimethylsilyl)-1-stibatetramethylcyclopentasilan-1-yl)zirconium Chloride (**10**).* KO*t*-Bu (12 mg, 0.111 mmol) and **5** (70 mg, 0.106 mmol) were dissolved in THF (2 mL) and stirred for 12 h (reaction control by NMR). The reaction mixture was cooled to −37 °C, and Cp_2ZrCl_2 (31 mg, 0.106 mmol) in THF (2 mL) was added slowly dropwise. After stirring for another 12 h complete conversion was achieved. Removal of solvent, treatment of the residue with pentane, filtration over Celite, and again removal of solvent caused the formation of some hydrostibine **4**. Crystallization from Et_2O afforded **10** (52 mg, 58%) as dark green crystals. Mp: 170−172 °C. ^1H NMR (δ ppm): 6.01 (s, 10H, Cp), 0.50 (s, 36H, $SiMe_3$), 0.44 (s, 12H, $SiMe_2$). ^{13}C NMR (δ ppm): 111.30 (Cp), 3.53 ($SiMe_3$), −1.13 ($SiMe_2$). ^{29}Si NMR (δ ppm): −8.1 ($SiMe_3$), −20.4 ($SiMe_2$), −103.7 (Si_q).

*Bis(cyclopentadienyl)(2,2,4,4-tetrakis(trimethylsilyl)-1-stibatetramethylcyclopentasilan-1-yl)hafnium Chloride (**11**).* Following the same procedure as described for **5**, using Mg (3 mg, 0.112 mmol), **2** (50 mg, 0.075 mmol), and Cp_2HfCl_2 (28 mg, 0.075 mmol), and addition of Cp_2HfCl_2 at −37 °C, the reaction was complete after 48 h. Black crystalline **11** (41 mg, 59%) was obtained by crystallization from Et_2O. As for the case of **10**, some hydrostibine **4** formation during isolation was observed but to a smaller degree. Mp: 138−140 °C. ^1H NMR (δ ppm): 5.81 (s, 10H, Cp), 0.51 (s, 36H, $SiMe_3$), 0.46 (s, 12H, $SiMe_2$). ^{13}C NMR (δ ppm): 110.58 (Cp), 3.55 ($SiMe_3$), −1.04 ($SiMe_2$). ^{29}Si NMR (δ ppm): −8.1 ($SiMe_3$), −19.9 ($SiMe_2$), −109.7 (Si_q). ^1H NMR (δ ppm, THF-D_2O capillary): 6.43 (s, 10H, Cp), 0.48 (s, 36H, $SiMe_3$), 0.45 (s, 12H, $SiMe_2$). ^{13}C NMR (δ ppm, THF-D_2O capillary): 111.07 (Cp), 3.05 ($SiMe_3$), −1.53 ($SiMe_2$). ^{29}Si NMR (δ ppm, THF-D_2O capillary): −8.1 ($SiMe_3$), −20.0 ($SiMe_2$), −111.3 (Si_q).

■ ASSOCIATED CONTENT

Ⓢ Supporting Information

Tables and CIF files containing crystallographic information for compounds **3**−**6**, **10**, and **11**. gHMBC ($^1H-^{29}Si$) and gHSQC ($^1H-^{13}C$) spectra and tabulated assignments of compound **9**. ^1H, ^{13}C, and ^{29}Si NMR spectra of compounds **3**, **6**, **8**, **10**, and **11**, for which no elemental analyses were obtained, are provided as measure of purity. This material is available free of charge via the Internet at http://pubs.acs.org.

■ AUTHOR INFORMATION

Corresponding Authors

*baumgartner@tugraz.at.

*christoph.marschner@tugraz.at.

Notes

The authors declare no competing financial interest.

■ ACKNOWLEDGMENTS

Support for this study was provided by the Austrian Fonds zur Förderung der wissenschaftlichen Forschung (FWF) via the projects P-22678 (C.M.) and P-25124 (J.B.). Dedicated to Dr. Vladimir V. Burlakov (A. N. Nesmeyanov Institute of Organoelement Compounds, Russian Academy of Sciences) on the occasion of his 60th birthday in recognition of his numerous accomplishments in group 4 metallocene chemistry.

■ REFERENCES

(1) Zitz, R.; Gatterer, K.; Reinhold, C. R. W.; Müller, T.; Baumgartner, J.; Marschner, C. *Organometallics*, **2015**, DOI: 10.1021/om501075v

(2) Becker, G.; Münch, A.; Witthauer, C. *Z. Anorg. Allg. Chem.* **1982**, *492*, 15−27.

(3) Becker, G.; Freudenblum, H.; Witthauer, C. *Z. Anorg. Allg. Chem.* **1982**, *492*, 37−51.

(4) Hitchcock, P. B.; Jones, C.; Nixon, J. F. *Angew. Chem., Int. Ed.* **1995**, *34*, 492−493.

(5) Durkin, J.; Hibbs, D. E.; Hitchcock, P. B.; Hursthouse, M. B.; Jones, C.; Jones, J.; Malik, K. M. A.; Nixon, J. F.; Parry, G. *J. Chem. Soc., Dalton Trans.* **1996**, 3277.

(6) Becker, G.; Eschbach, B.; Mundt, O.; Reti, M.; Niecke, E.; Issberner, K.; Nieger, M.; Thelen, V.; Nöth, H.; Waldhör, R.; Schmidt, M. *Z. Anorg. Allg. Chem.* **1998**, *624*, 469−482.
(7) Gröer, T.; Scheer, M. *J. Chem. Soc., Dalton Trans.* **2000**, 647−653.
(8) Weber, L.; Mast, C. A.; Scheffer, M. H.; Schumann, H.; Uthmann, S.; Boese, R.; Bläser, D.; Stammler, H.-G.; Stammler, A. *Z. Anorg. Allg. Chem.* **2000**, *626*, 421−429.
(9) Von Hänisch, C.; Scheer, P.; Rolli, B. *Eur. J. Inorg. Chem.* **2002**, *2002*, 3268−3271.
(10) Bruce, S.; Hibbs, D. E.; Jones, C.; Steed, J. W.; Thomas, R. C.; Williams, T. C. *New J. Chem.* **2003**, *27*, 466−474.
(11) Jones, C.; Thomas, R. C. *J. Organomet. Chem.* **2001**, *622*, 61−65.
(12) Marschner, C. *Eur. J. Inorg. Chem.* **1998**, 221−226.
(13) Kayser, C.; Fischer, R.; Baumgartner, J.; Marschner, C. *Organometallics* **2002**, *21*, 1023−1030.
(14) Marschner, C. *Organometallics* **2006**, *25*, 2110−2125.
(15) Noblet, P.; Cappello, V.; Tekautz, G.; Baumgartner, J.; Hassler, K. *Eur. J. Inorg. Chem.* **2011**, 101−109.
(16) Ishida, S.; Hirakawa, F.; Furukawa, K.; Yoza, K.; Iwamoto, T. *Angew. Chem., Int. Ed.* **2014**, *53*, 11172−11176.
(17) Herbstman, S. *J. Org. Chem.* **1964**, *29*, 986−987.
(18) Zhang, L.-J.; Huang, Y.-Z. *J. Organomet. Chem.* **1993**, *454*, 101−103.
(19) Westerhausen, M.; Gückel, C.; Piotrowski, H.; Mayer, P.; Warchhold, M.; Nöth, H. *Z. Anorg. Allg. Chem.* **2001**, *627*, 1741−1750.
(20) Breunig, H. J. *Z. Naturforsch., B* **1978**, *33*, 242−243.
(21) Breunig, H. J.; Severengiz, T. *Z. Naturforsch., B* **1982**, *37*, 395−400.
(22) Fischer, R.; Frank, D.; Gaderbauer, W.; Kayser, C.; Mechtler, C.; Baumgartner, J.; Marschner, C. *Organometallics* **2003**, *22*, 3723−3731.
(23) Fischer, R.; Konopa, T.; Baumgartner, J.; Marschner, C. *Organometallics* **2004**, *23*, 1899−1907.
(24) Breunig, H. J.; Ghesner, M. E.; Lork, E. *Z. Anorg. Allg. Chem.* **2005**, *631*, 851−856.
(25) Breunig, H. J.; Moldovan, O.; Nema, M.; Rosenthal, U.; Rat, C. I.; Varga, R. A. *J. Organomet. Chem.* **2011**, *696*, 523−526.
(26) Breunig, H. J.; Lork, E.; Moldovan, O.; Raţ, C. I.; Rosenthal, U.; Silvestru, C. *Dalton Trans.* **2009**, 5065−5067.
(27) Breunig, H. J.; Borrmann, T.; Lork, E.; Raţ, C. I.; Rosenthal, U. *Organometallics* **2007**, *26*, 5364−5368.
(28) Waterman, R.; Tilley, T. D. *Inorg. Chem.* **2006**, *45*, 9625−9627.
(29) Waterman, R.; Tilley, T. D. *Chem. Commun.* **2006**, 4030−4032.
(30) Waterman, R.; Tilley, T. D. *Angew. Chem., Int. Ed.* **2006**, *45*, 2926−2929.
(31) Wade, S. R.; Wallbridge, M. G. H.; Willey, G. R. *J. Organomet. Chem.* **1984**, *267*, 271−276.
(32) Krempner, C. *Polymers* **2012**, *4*, 408−447.
(33) Breunig, H. J.; Ghesner, M. E.; Lork, E. *J. Organomet. Chem.* **2002**, *660*, 167−172.
(34) Westerhausen, M.; Gückel, C.; Warchhold, M.; Nöth, H. *Organometallics* **2000**, *19*, 2393−2396.
(35) Balázs, G.; Breunig, H. J.; Lork, E.; Mason, S. *Organometallics* **2003**, *22*, 576−585.
(36) Twamley, B.; Hwang, C.-S.; Hardman, N. J.; Power, P. P. *J. Organomet. Chem.* **2000**, *609*, 152−160.
(37) Conquest, version 1.16 was used. Bruno, I. J.; Edgington, P. R.; Kessler, M.; Macrae, C. F.; McCabe, P.; Pearson, J.; Taylor, R. *Acta Crystallogr., Sect. B* **2002**, *58*, 389−397.
(38) Cappello, V.; Baumgartner, J.; Dransfeld, A.; Hassler, K. *Eur. J. Inorg. Chem.* **2006**, 4589−4599.
(39) Pangborn, A. B.; Giardello, M. A.; Grubbs, R. H.; Rosen, R. K.; Timmers, F. J. *Organometallics* **1996**, *15*, 1518−1520.
(40) Morris, G. A.; Freeman, R. *J. Am. Chem. Soc.* **1979**, *101*, 760−762.
(41) Helmer, B. J.; West, R. *Organometallics* **1982**, *1*, 877−879.
(42) *SAINTPLUS: Software Reference Manual*, version 6.45; Bruker-AXS: Madison, WI, 1997-2003.
(43) Sheldrick, G. M. *SADABS*, version 2.10; Bruker-AXS: Madison, WI, 2003.
(44) Sheldrick, G. M. *Acta Crystallogr., Sect. A* **2007**, *64*, 112−122.

DOI: 10.1021/om501297h
Organometallics 2015, 34, 1431−1439